(Received 13 November 2025, Accepted 21 January 2026, Scheduled 14 March 2026)

Large-Scale Grounding System Modeling and Characteristics Analysis in Urban Underground Utility Tunnels

Shangmao Hu[1, 2], Yasong Cao[3, *], and Wen Cao[3]

[1]*Electric Power Research Institute, China Southern Power Limited Company, Guangdong 510663, China*
[2]*National Engineering Research Center of UHV Technology and Novel Electrical Equipment Basis, Guangdong 510663, China*
[3]*School of Electronic Information, Xi'an Polytechnic University, Xi'an 710048, China*

ABSTRACT: The coupling of extensive metallic components within utility tunnels significantly complicates the earth-entry and dispersion pathways of cable short-circuit fault currents. This study focuses on a conventional three-compartment utility tunnel to guarantee steady and dependable operation of transmission lines. An integrated grounding system model with a concrete shell, vertical grounding electrodes, and grounding busbar bonding was constructed under various soil-resistivity conditions. The effects of bonding distance, vertical grounding electrode arrangement, and resistivity of the concrete shell on the grounding resistance, ground potential rise, touch voltage, and step voltage were methodically investigated by parametric simulations using CDEGS software. The findings indicate that an appropriate grounding grid spacing can significantly improve the electrical properties of the grounding system, whereas excessive density diminishes these advantages owing to the reciprocal coupling. The incorporation and deepening of the vertical grounding electrodes significantly diminished the ground resistance and ground potential rise. As the resistivity of the concrete shell increased, both the equivalent electrical parameters and surface potential gradient increased markedly. Research has shown that the interaction between the grounding network in utility tunnels and the adjacent soil influences fault-current dispersion pathways. This study provides a reference for optimizing the design of grounding systems for utility tunnels.

1. INTRODUCTION

Urban subterranean utility tunnels, which are essential for contemporary city infrastructure, are pivotal in new urbanization strategies. By consolidating telecommunications, water supply, drainage, and other utility lines within a single subterranean space, the efficiency of urban spatial resource utilization is markedly improved [1, 2]. The "multi-line co-chamber" configuration not only bolsters the integrity and coordination of urban infrastructure but also offers distinct benefits in augmenting overall disaster resistance and increasing urban landscape aesthetics. This has become a crucial component in the development of contemporary smart cities.

Nevertheless, the complex underground spatial structure and dense metal components of underground utility tunnel grounding systems produce significantly different fault current dispersion paths compared to traditional above-ground substations in the design and operation of these systems. This unique environment has the potential to result in abnormal ground resistance and uneven ground potential distribution, which can directly imperil the safety of maintenance personnel by causing step and touch voltages to exceed safety limits [3]. Consequently, conducting focused research on the characteristics of the grounding current dispersion is of substantial practical value in the context of ensuring the safe operation of utility tunnel power systems.

Currently, scholars predominantly use the finite element method, hemispherical electrode models, and resistive network models to conduct in-depth analyses of stray current distribution patterns and corresponding protective measures [4]. Charalambous et al. introduced the concept of stray current leakage rate to comprehensively investigate the current distribution under multiple influencing factors [5, 6]. Bortels et al. investigated the characteristics of leakage currents using an extended field theory model [7], whereas Cerman et al. conducted stray current distribution modeling and analysis from the resistive network perspective [8]. Simultaneously, international research has concentrated on the corrosion effects of stray currents, utilizing electrochemical methodologies to assess the durability of reinforced concrete structures and to create dynamic prediction models that are based on multi-physics coupling [9–11]. Substantial advancements have been made in domestic research. Yin et al. conducted research on the detection and protection of stray currents in the subways [12–14]. The influence patterns of transition resistors on stray currents were validated by Zhu et al. using CDEGS software [15]. In recent years, there has been a growing trend in research that prioritizes multi-factor coupled analysis. For example, Zhuang et al. investigated the degradation mechanisms of concrete under intricate environmental conditions by investigating the combined effects of stray currents and salt-freeze cycles [16].

Regarding current research on grounding systems for cable tunnels and gas-insulated transmission line (GIL) tunnels, Song et al. analyzed the impact of grounding resistance and connection configurations on cable fault overvoltage [17]. However, their study was based on a lumped parameter model and

* Corresponding author: Yasong Cao (1650228570@qq.com).

did not thoroughly investigate the spatial influence of complex tunnel structures on fault current dissipation paths. Li et al. proposed a computational model for the electromagnetic coupling between GIL conductors and their enclosures [18]. However, this model was primarily intended for electromagnetic transient calculations and did not address the physical field distribution of the grounding grid or the specific assessment of personnel safety indices in a multi-medium environment. Tang et al. conducted a comprehensive study on the influence of GIL utility tunnel structures on the electrical characteristics of grounding systems [19]. Yet, their work was limited to a single-compartment GIL utility tunnel and did not extend to the analysis of multi-compartment urban utility tunnels. Similarly, the team led by Fan investigated the grounding characteristics of transmission pipelines in mountainous regions with high soil resistivity, but their conclusions are applicable only to that specific geographic terrain [20].

In summary, current research primarily focuses on the grounding characteristics of surface substations and traditional single-compartment cable tunnels. While some studies have explored the electrical properties of GIL utility tunnels, they are largely confined to single physical structures or rely on the simplified assumptions of uniform, semi-infinite soil space. However, urban underground utility tunnels possess a unique "multi-compartment" physical structure. The compartments are isolated by concrete shells that exhibit shielding efficacy, and the interiors are densely distributed with metallic components, such as support brackets and grounding busbar. This complex multi-medium environment, which constitutes a "soil-concrete-metal network", results in fault current dissipation paths and current shunting coefficients that are fundamentally distinct from those of traditional direct-buried cables or single-compartment tunnels. Existing simplified models fail to accurately characterize the combined impact of the concrete shell's resistivity variations and the intricate internal equipotential bonding network on ground potential distribution. Consequently, systematic research into the dissipation mechanisms of such large-scale, complex underground systems remains insufficient.

Therefore, to systematically analyze this complex structure, this study focuses on a typical urban three-compartment utility tunnel. We have constructed a refined simulation model that incorporates the concrete shell, the electrically continuous reinforcement network, and the interconnection relationships of various metallic components. In contrast to previous studies that focused solely on single structures, this work conducts a systematic analysis of the grounding system's electrical characteristics. Furthermore, we place a particular emphasis on quantifying the impact of key structural parameters on grounding resistance and surface potential gradients (i.e., touch and step voltages). We focus specifically on factors that have received limited attention in earlier literature, including the resistivity of the concrete shell, the interconnection topology of metal components, and the cross-bonding spacing of grounding busbars. By revealing the current dissipation mechanisms under multi-factor coupling, this study aims to provide clear quantitative guidance and engineering recommendations for the optimized design of large-scale grounding systems in multi-compartment utility tunnels.

2. COMPREHENSIVE UTILITY TUNNEL MODEL AND GROUNDING SYSTEM MODELING

2.1. Structure of a Typical Three-Compartment Integrated Utility Tunnel

The research subject of this investigation is a typical three-compartment utility tunnel. The 1-km-long tunnel has an external width of 8 m and an overall height of 4.05 m, and is buried 3 m below ground level. The concrete shell was composed of a 0.4 m-thick top slab, a 0.45 m-thick bottom slab, and 0.4 m-thick side walls. The walls were internally reinforced with 16 mm-diameter structural reinforcing steel. The compartments are the locations of communication cables, low-voltage cables, and high-voltage cables, metal brackets (C-channel steel) that are affixed to the sidewalls to ensure that all cables are securely connected to the compartment's grounding busbar. Figure 1 illustrates a schematic cross-section of the utility conduit.

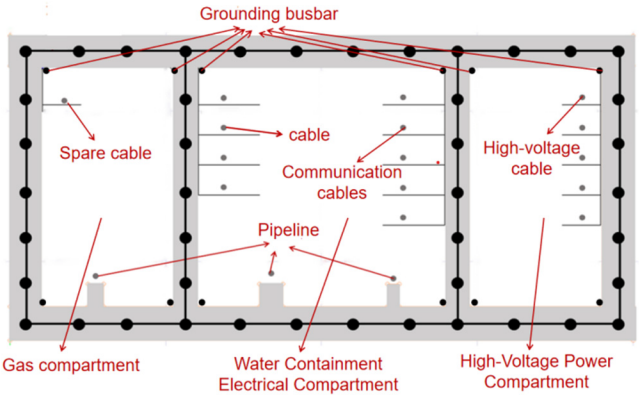

FIGURE 1. Schematic cross-section of utility tunnel.

The grounding system primarily employs a natural grounding body created by a structural reinforcing steel. This body is composed of a bottom slab, side walls, and top slab reinforcement, which are reliably interconnected to form a three-dimensional closed network. This network was equivalent to a dense grid electrode. In each compartment, two copper grounding busbars (50 mm $\times$ 4 mm) were installed at the top corners (ceiling-wall junctions). Internal jumpers were installed at regular intervals within the compartments, and jumpers were installed between adjacent compartments. At least two grounding leads connect the structural steel ring grounding network to both extremities of the grounding busbar. Equipotential bonding with the top copper grounding busbar was achieved by the primary structural steel ring network approximately every 100 m. This creates a continuous, low-resistance grounding network with clearly defined equipotential relationships by incorporating structural reinforcing steel, metal brackets, metal conduits, grounding busbars, and necessary outerring conductors. This enables the rapid dissipation of fault currents into the Earth and results in a more uniform surface potential distribution, thereby reducing the touch voltage and step voltage.

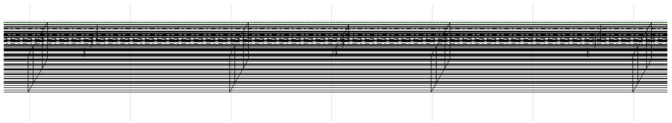

FIGURE 2. Overall schematic diagram of the utility tunnel grounding system.

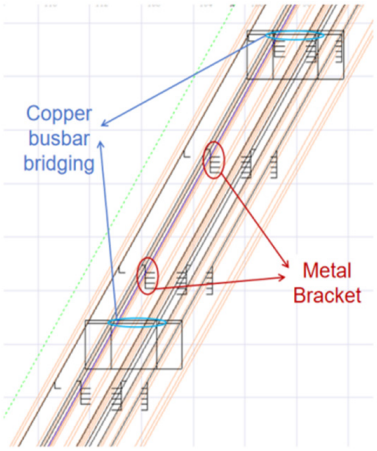

FIGURE 3. Partial schematic representation of utility tunnel.

2.2. Modeling and Parameter Configuration of Grounding Systems

A three-compartment utility tunnel grounding system model was developed using CDEGS, as shown in Figure 2, based on previously specified structural conditions. A partial schematic of the utility tunnel model is shown in Figure 3 for enhanced clarity and intuitiveness. In the modeling process, the structural reinforcing steel mesh was divided into equidistant grids to define the corresponding grid electrode characteristics. Significant attention has been directed towards considering the mutual impedance and mutual inductance between adjacent main bars aligned in the same direction, as well as between the supplementary ring-shaped flat steel/copper grounding busbars installed along the line, owing to their influence on the current distribution and surface potential gradients. To optimize the current dispersion, the horizontal space between the superimposed artificial grounding electrodes or outer ring conductors was maintained at a minimum of 5 m to mitigate shielding effects and improve the uniformity of the current distribution.

Natural grounding bodies, specifically structural reinforcing steel, are represented as cohesive equipotential networks comprising the grounding busbars, outer ring conductor, and grounding leads. Designated equipotential connection sites and test points were developed to regulate connection resistance and continuity. The parameters for conductors are delineated as follows: grounding busbar, jumpers, and grounding leads utilize $50\,\text{mm} \times 4\,\text{mm}$ rectangular copper grounding busbar; the diameter of the primary structural reinforcing steel is 16 mm. Concerning connection organization, the compartments grounding the busbar utilize equidistant bonding and establish connectivity between neighboring compartments. At intervals of approximately 100 meters along the route, the copper grounding busbar at the upper bend is interconnected with the structural reinforcing steel ring network to establish equipotential bonding. It establishes a continuous, low-resistance grounding network with uniform potential distribution along the entire pathway.

Based on the aforementioned three-compartment integrated utility tunnel model, a 10 kA short-circuit excitation current is applied at the initial section of the high-voltage cable to simulate a fault condition, thereby calculating the electrical characteristic parameters of the grounding system. This study primarily investigates the impact of the concrete shell and the complex internal structures of utility tunnels on the electrical characteristics of the grounding system within complex underground environments, under the condition of a constant short-circuit current magnitude.

3. THE IMPACT OF VARIED SOIL CONDITIONS ON ELECTRICAL CHARACTERISTIC PARAMETERS

3.1. Impact of Soil Resistivity

The soil conditions in underground utility tunnels significantly affect the trajectory and magnitude of the fault current distribution [21]. High-resistivity soils markedly increase the ground potential rise, directing fault currents to discharge largely through metallic components. In contrast, low-resistivity soils enable a wider current distribution, diminishing the current density at specific locations while potentially enlarging the impacted region. Consequently, in the design of grounding systems and stray current prevention, it is imperative to incorporate soil survey findings to judiciously choose the configuration and materials of grounding electrodes. Enhanced insulation or cathodic protection methods must be employed under high-risk soil conditions to provide optimal protection efficacy [22].

To examine the influence of different soil resistivity conditions on the electrical properties of the grounding systems, the following subsequent critical parameters were defined: the distance between the metal bracket was established at 20 m; the resistivity of the concrete shell was determined to be $2000\,\Omega \cdot \text{m}$; and soil resistivities were sequentially assigned values of $50\,\Omega \cdot \text{m}$, $100\,\Omega \cdot \text{m}$, $200\,\Omega \cdot \text{m}$, $300\,\Omega \cdot \text{m}$, $500\,\Omega \cdot \text{m}$, and $1000\,\Omega \cdot \text{m}$. The span of the grounding busbar was set to 100 m. A simulation analysis was performed on the grounding resistance, touch voltage, step voltage, ground potential rise of the complete grounding system considering, and the influence of soil resistivity on current dispersion. The findings are summarized in Table 1.

The electrical characteristics of the grounding system for urban underground utility tunnels are substantially influenced by variations in the soil resistivity, as evidenced by the data presented in Table 1. The grounding resistance increased from $0.0963\,\Omega$ to $1.5587\,\Omega$ as the soil resistivity progressively increased from $50\,\Omega \cdot \text{m}$ to $1000\,\Omega \cdot \text{m}$, a rise that exceeded 15 times. In tandem, the ground potential increased from 894.509 to 15312 V, which is an approximately 16-fold increase. This suggests a distinct negative correlation between the performance of the grounding system and the soil resistivity.

The touch voltage increased from 294.535 to 4037.642 V, while the step voltage increased from 27.201 to 391.454 V in terms of voltage distribution. Elevated soil resistivity substan-

TABLE 1. Electrical property parameters under varied soil conditions.

Soil resistivity/Ω · m	Ground resistance/Ω	Step voltage/V	Touch voltage/V	Ground potential rise/V
50	0.0963	27.201	294.535	894.509
100	0.1773	47.126	539.509	1673.611
200	0.3309	98.300	949.565	3162.950
300	0.4832	114.015	1195.871	5089.179
500	0.7929	180.551	1824.510	7718.116
1000	1.5587	391.454	4037.642	15312

TABLE 2. Parameters for each layer in the new stratification.

Serial Number	Stratification	Thickness/m	Resistivity/Ω · m	Relative Permittivity
1	air layer	∞	1×10^{18}	1
2	road surface	0.1	3000	6
3	topsoil layer	2.4	180	9
4	deep soil layers	∞	300	20

tially amplifies surface potential gradients, thereby adversely affecting system operational safety, as evidenced by these increases, which exceed 13-fold and 12-fold, respectively. In terms of current diffusion behavior, lower soil resistivity enables a more uniform dispersion of current through deeper soil layers, resulting in the formation of broader, low-impedance current paths. This assists in the reduction of the grounding resistance and suppression of the surface potential rise. In contrast, current diffusion is restricted by high soil resistivity, which results in current concentration and exacerbated potential gradients. Consequently, the influence of soil resistivity must be meticulously evaluated during the development and optimization of utility tunnel grounding systems. Prioritizing the selection of low-resistivity areas or the implementation of resistivity reduction measures to improve the current dispersion efficiency and safety performance of the system should be prioritized when conditions allow.

3.2. Impact of Soil Stratification

The critical component that guarantees long-term durability and overall structural stability during the actual construction process is the reinforced concrete box structure of utility tunnels, which includes the base slab, side walls, and roof slab. Additionally, the tunnel structure is typically encircled by backfill soil or in-situ soil layers, with the upper section typically covered by a road structure system that frequently includes concrete pavement or cement-stabilized pulverized stone base layers. In electrical characteristic analysis, these materials can be utilized as high-resistance covering layers owing to their high electrical resistivity. Consequently, the concrete structural layer and its adjacent soil must be regarded as stratified media during the grounding and potential distribution analysis. Considering the aforementioned factors, structural data, and soil conditions of a particular utility tunnel project, the schematic diagram depicted in Figure 4 was created.

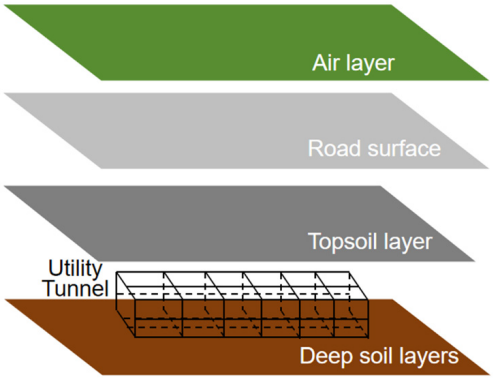

FIGURE 4. Schematic diagram of stratified soil.

The thickness, resistivity, and relative permittivity of each layer were determined after refining the soil into distinct strata. The data presented in Table 2 are utilized for the simulation analysis. Tables 2 and 3 illustrate a comparison between the original data and the results obtained. Furthermore, while the thickness and resistivity of soil layers do exert a certain influence on the electrical characteristic parameters, they are not elaborated upon in detail here.

The layered soil model is in accordance with engineering realities, as evidenced by the data in Table 3. The electrical characteristics of the grounding system were generally slightly elevated when layering was not considered. Adopting the layered soil model results in a 5.16% reduction in the ground resistance from 0.1550 Ω to 0.1470 Ω compared to the non-layered model. Additionally, the ground potential rise decreased from 1520.299 to 1453.494 V, a 4.39% reduction. The layered structure's ability to suppress surface potential gradients and improve system safety is evidenced by the 12.21% and 16.69% decreases in step voltage and touch voltage, respectively, in terms of safety metrics.

TABLE 3. Comparison of electrical characteristic parameters before and after soil stratification.

	Ground resistance/Ω	Step voltage/V	Touch voltage/V	Ground potential rise/V
Unstratified	0.1550	35.527	310.296	1520.299
Stratification	0.1470	31.189	258.517	1453.494
Percentage Change Rate%	−5.16%	−12.21%	−16.69%	−4.39%

TABLE 4. Effect of resistivity of concrete shell on electrical characteristic parameters.

Resistivity of concrete shell/Ω · m	Ground resistance/Ω	Step voltage/V	Touch voltage/V	Ground potential rise/V
1000	0.1698	42.251	470.709	1613.244
2000	0.1773	47.126	539.509	1673.611
3000	0.1831	50.792	576.034	1726.268
5000	0.1936	56.834	840.159	1830.424
8000	284.603	284.603	2697.378	2063.224

The current distribution pattern in the original homogeneous medium is altered by the layered soil from the perspective of current diffusion pathways, resulting in fault currents preferentially diffusing along low-resistance layers. This enhances grounding efficacy by optimizing the current dispersion path. The results suggest that the integration of soil stratification characteristics into the design of utility tunnel grounding systems facilitates a more precise evaluation of system performance and establishes a dependable foundation for engineering safety design.

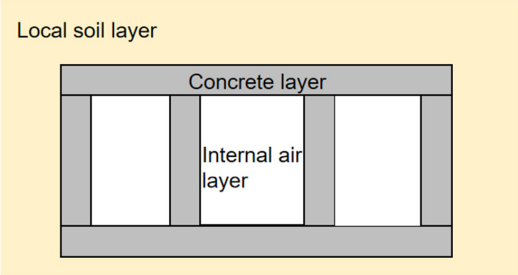

FIGURE 5. Concrete shell model diagram.

4. THE EFFECT OF CONCRETE STRUCTURAL SHELLS ON ELECTRICAL CHARACTERISTIC PARAMETERS

4.1. Effect of Resistivity of Concrete Shell

The interface impedance through which the fault current couples from the internal grounding network to the surrounding soil is determined by the concrete exterior of the utility tunnel, which is a covering layer connected in series with the soil. The resistivity of the concrete shell ranges from 10^2–10^4 Ω · m as a result of the moisture content in the adjacent soil environment and the mix proportions [23].

This variation affects the surface potential gradient and equivalent path length of the current entering the soil. To investigate the influence of concrete shell resistivity on the electrical characteristics of the grounding system, simulation calculations were conducted under the following conditions: a soil resistivity of 100 Ω · m and a grounding busbar bonding interval of 100 m. The specific results are listed in Table 4. Figure 5 presents a schematic diagram of the concrete shell model.

The electrical characteristics of the utility tunnel grounding system are substantially influenced by changes in the resistivity of the concrete shell, as indicated by the simulation data presented in Table 4. The grounding resistance increased by 27.4% from 0.1698 Ω to 0.2164 Ω as the concrete shell resistivity increased from 1000 Ω · m to 8000 Ω · m. Consequently, the ground potential rise increased from 1613.244 V to 2063.224 V, indicating a 27.9% increase. The touch voltage increased from 470.709 V to 2697.378 V, a 473.1% increase, while the step voltage surged from 42.251 V to 284.603 V, representing a 573.6% increase, in terms of safety metrics. This illustrates that the surface potential gradients are substantially amplified by high-resistivity concrete structures, which have severe adverse effects on system safety.

The concrete shell is a critical medium, through which fault currents penetrate soil from the perspective of current diffusion pathways. Currents are compelled to concentrate more intensely along metallic pathways, such as grounding busbars, because of an increase in their resistivity, which impedes lateral current diffusion. This results in a heightened local current density, which exacerbates the surface potential gradients and increases the grounding resistance. According to the research findings, the resistive characteristics of the concrete shell must be thoroughly considered when grounding systems are designed for utility tunnels. The overall current dispersion efficiency and safety performance of the system can be improved by optimizing material selection or structural design to control its resistivity.

TABLE 5. Effect of adding vertical ground electrodes on electrical characteristics parameters.

Vertical ground electrode spacing/m	Ground resistance/Ω	Step voltage/V	Touch voltage/V	Ground potential rise/V
No additions	0.1773	47.126	539.509	1673.611
1000	0.1695	38.594	479.655	1597.189
200	0.1668	38.582	453.075	1590.748
100	0.1655	38.020	430.815	1579.056
50	0.1642	37.798	415.655	1570.451

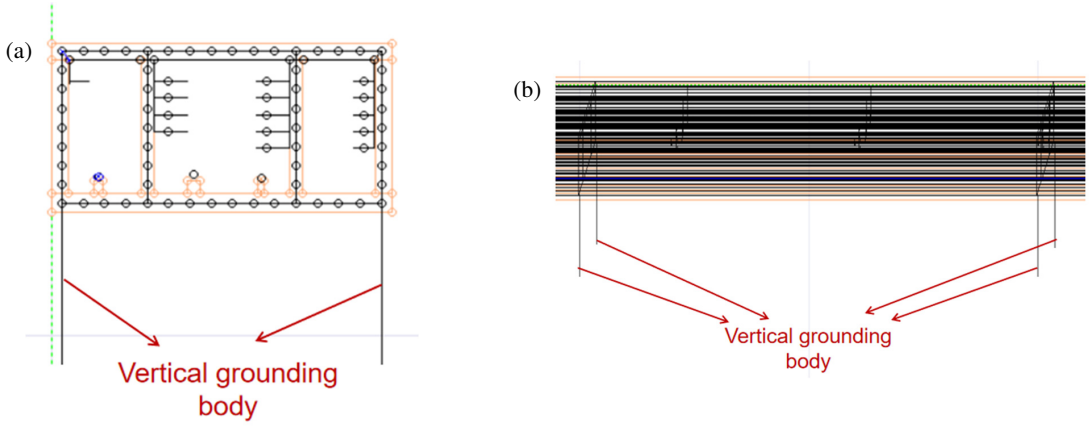

FIGURE 6. Vertical grounding electrode installation. (a) Front view. (b) Side view.

4.2. Effect of Adding Vertical Ground Electrodes

In utility tunnels, the spatial distribution and dissipation of fault currents can be considerably enhanced by the installation of vertical grounding electrodes, in addition to the horizontal grounding grid and equalization strip, in the grounding system. Vertical grounding electrodes penetrate high-resistance backfill layers or concrete casings to access deep, low-resistance soil strata. This effectively expands the effective grounding cross-section, reduces the equivalent ground resistance, and distributes the current density near the surface by providing multiple depth-dependent pathways for current entry into the ground.

In practical engineering, it is common for multiple vertical grounding electrodes to be arranged in groups and connected in parallel to a horizontal grid. Deployment of these devices is prioritized in areas with a high concentration of equipment, corners, and current injection points. Mutual interference effects are suppressed through rational control of the electrode length and spacing, resulting in a more optimal equilibrium among "current dispersion, voltage equalization, and resistance reduction". Figure 6 illustrates the simulated arrangement of perpendicular grounding electrodes. To investigate the influence of the number of vertical grounding electrodes on the electrical characteristics of the grounding system, simulation calculations were conducted under the following conditions: a soil resistivity of 100 Ω · m, a concrete shell resistivity of 2000 Ω · m, and a grounding busbar bonding interval of 100 m. The specific results are presented in Table 5.

The electrical characteristics of the utility tunnel grounding system were considerably enhanced by the addition of vertical grounding electrodes and their spacing settings, as indicated by the simulation data in Table 5. The system grounding resistance decreased steadily from 0.1773 Ω to 0.1642 Ω as the spacing between the vertical electrodes progressively decreased from 1000 m to 50 m, compared to the baseline condition without vertical grounding electrodes. This represents a cumulative reduction of 7.4%. Subsequently, the ground potential surge decreased from 1673.611 to 1570.451 V, which is equivalent to a 6.2% decrease. The step voltage decreased from 47.126 to 37.798 V, representing a 19.8% decrease in the safety metrics. A 22.9% decrease was observed in the touch voltage, which plummeted from 539.509 V to 415.655 V. This illustrates the successful suppression of the surface potential gradients achieved by the vertical grounding electrodes.

The introduction of vertical grounding electrodes alters the original horizontal-dominant current dispersion pattern by providing a low-resistance channel for fault currents to diffuse into deeper soil layers from the perspective of current diffusion pathways. The current density near the ground surface is effectively reduced by the "three-dimensional" dispersion structure, which also directs the current distribution vertically, thereby reducing the grounding resistance of the system. As a result, the step voltage and touch voltage levels were significantly enhanced. The rational configuration of vertical grounding electrodes in the design of utility tunnel grounding systems is an effective technical measure to improve the current dispersion efficiency and safety performance of the system.

TABLE 6. Influence of the bridging distance of the grounding busbar in the same compartment on electrical characteristic parameters.

Grounding busbar bridge distance/m	Step voltage/V	Touch voltage/V	Ground potential rise/V
200	47.540	544.835	1688.760
100	47.126	539.509	1673.611
80	46.709	522.901	1650.601
50	43.641	423.714	1622.166
20	43.021	416.915	1570.436

5. EFFECT OF METAL BONDING IN UTILITY TUNNELS ON ELECTRICAL CHARACTERISTIC PARAMETERS

5.1. Impact of Grounding Busbar Bonding

The formation of closed circuits through interconnected metal components in the electrical design of utility tunnels can effectively improve the fault current dispersion. Nevertheless, the number of loops increases, resulting in a greater number of copper bus cross-connections and connection points, which, in turn, substantially increases the costs of material and construction. Consequently, the design must rationally plan the layout and density of the current dispersion paths to achieve a balance between safety and economy.

To investigate the influence of the grounding busbar bonding interval on the electrical characteristics of the grounding system, simulation calculations were conducted under the following conditions: a soil resistivity of 100 Ω · m, a concrete shell resistivity of 2000 Ω · m, without the installation of vertical grounding electrodes. The objective was to determine an appropriate bonding interval. The specific results are listed in Table 6.

Based on the simulation data provided in Table 6 and Figure 7, variations in the bonding interval of the grounding busbar within the compartment significantly influence the electrical characteristics of the utility tunnel's grounding system. As the bonding interval is progressively reduced from 200 m to 20 m, the grounding resistance exhibits a continuous downward trend, decreasing from 0.1779 Ω to 0.1587 Ω. Concurrently, the efficacy of resistance reduction is progressively enhanced as the interval shortens. From the perspective of resistance reduction performance, the 20 m interval achieves an 11.83% reduction compared to the 200 m scenario. Notably, the improvement is most pronounced within the range of 80 m to 50 m. This indicates that a rationally selected bonding interval can effectively optimize the performance of the utility tunnel grounding system.

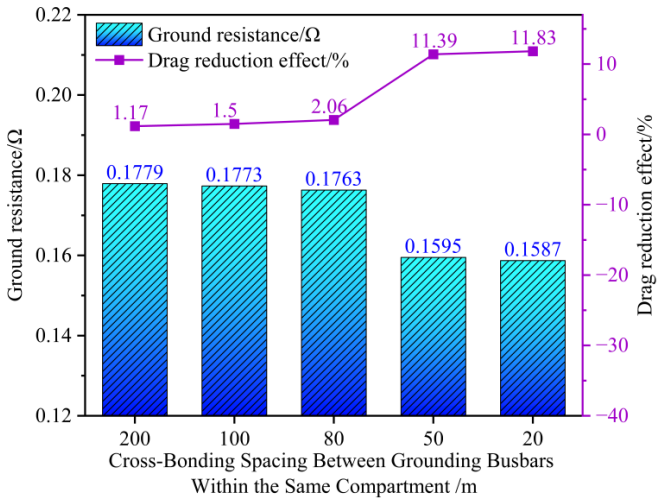

FIGURE 7. Effect of cross-bonding spacing between grounding busbars within the same compartment on grounding resistance.

The ground potential rise also exhibited a downward trend, decreasing from 1688.760 to 1570.436 V, a 7.0% reduction. The step voltage decreased from 47.540 V to 43.021 V in terms of safety metrics, a 9.5% decrease. The touch voltage experienced a substantial decrease, dropping from 544.835 to 416.915 V, resulting in a 23.5% reduction. This illustrates the efficacy of decreasing the jumper distance to enhance the surface potential distribution.

The formation of a denser grid-like current dispersion network is facilitated by the appropriate reduction in the bonding distance from the perspective of current dispersion pathways. This optimizes the grounding performance by promoting the uniform, multi-path diffusion of fault currents. The system obtains an optimal balance between the current dispersion efficiency and engineering economics within a bonding distance range of 50–80 m, according to the research findings. This is an essential reference for the design of the grounding busbars in integrated utility pipelines.

5.2. Impact of Grounding Busbar and Main Structural Reinforcing Steel Bonding

To investigate the influence of the bonding interval between the grounding busbar and the main structural reinforcement on the electrical characteristics of the grounding system, simulation calculations were conducted under the following conditions: a soil resistivity of 100 Ω · m, a concrete shell resistivity of 2000 Ω · m, and a grounding busbar bonding interval of 100 m, without the installation of vertical grounding electrodes. The objective was to determine an appropriate bonding interval. The specific results are listed in Table 7.

Based on the simulation data presented in Table 7 and Figure 8, variations in the bonding interval between the grounding busbar and the main structural reinforcement significantly

TABLE 7. Impact of grounding busbar and main structural reinforcing steel bonding on electrical characteristic parameters.

Crossover distance/m	Step voltage/V	Touch voltage/V	Ground potential rise/V
1000	47.126	539.509	1673.611
200	44.378	526.288	1657.208
100	43.641	520.461	1644.061
50	42.511	514.218	1626.201
20	41.884	495.183	1592.910

influence the electrical characteristics of the utility tunnel's grounding system. As the bonding interval is progressively reduced from 1000 m to 20 m, the grounding resistance exhibits a continuous downward trend, decreasing from 0.1773 Ω to 0.1702 Ω. Concurrently, the efficacy of resistance reduction within the grounding system progressively improves as the interval shortens. From the perspective of resistance reduction performance, the 20 m interval achieves an improvement of approximately 5.44% compared to the 1000 m scenario. This indicates that shortening the bonding interval between the grounding busbar and the main structural reinforcement is conducive to enhancing the overall resistance reduction performance of the grounding system.

A dense conductive network is formed by the close connection between the grounding trunk and the primary structural reinforcing steel from the perspective of current dispersion pathways. This promotes uniform current diffusion by providing additional low-resistance paths for fault currents to flow through. Structural reinforcing steel becomes more actively involved in the current dispersion process as the bonding distance decreases, thereby expanding the dispersion range and optimizing system performance. Research suggests that the safety and dispersion efficiency of the grounding system can be substantially improved by restricting the bonding distance to approximately 20 m.

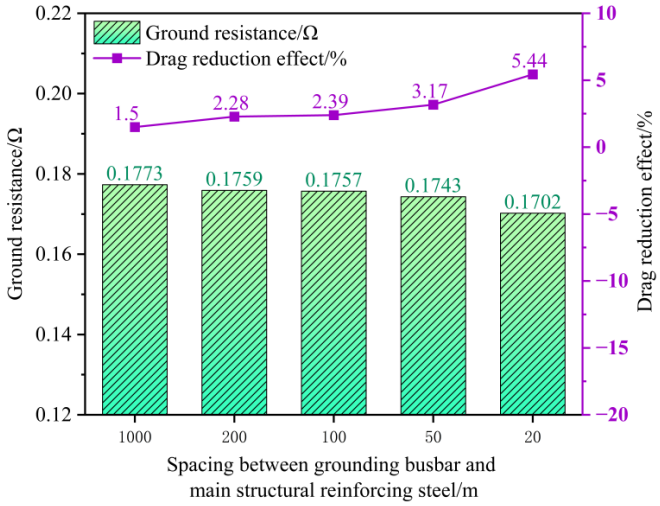

FIGURE 8. Effect of spacing between grounding busbar and main structural reinforcing steel on grounding resistance.

6. CONCLUSION

This paper systematically investigates the current dissipation mechanism and influencing factors of urban underground three-compartment utility tunnels under short-circuit conditions. By establishing a refined integrated model that combines structural reinforcement, internal metallic components, and the concrete shell within a stratified soil environment, this study quantifies the impact of key parameters on the grounding system and safety indices. Consequently, the following conclusions are drawn:

(1) The simulation results quantify the high sensitivity of the utility tunnel's grounding performance to soil resistivity. Both grounding resistance and Ground Potential Rise (GPR) exhibited an order-of-magnitude increase as soil resistivity rose from 50 Ω · m to 1000 Ω · m. However, compared to the uniform soil model, the stratified soil scenarios demonstrated a reduction in these electrical parameters, validating the enhanced current diffusion capability facilitated by low-resistivity layers in the deep soil.

(2) The concrete shell functions as a critical resistive barrier that impedes current diffusion. Increasing the shell resistivity from 1000 Ω · m to 8000 Ω · m resulted in a significant increase across all electrical characteristic parameters. This indicates that a high-resistivity shell intensifies the shielding effect, inhibiting current dissipation into the surrounding soil and constraining fault currents within the internal metallic pathways. This underscores the necessity of accounting for the concrete shell in safety designs.

(3) Vertical grounding electrodes serve as effective channels for penetrating high-resistivity concrete barriers. Reducing the installation interval from 1000 m to 50 m resulted in reductions of 19.8% and 22.9% in step voltage and touch voltage, respectively. However, a saturation effect is observed with the increased density of vertical electrodes. Due to the mutual shielding effect, the marginal benefit diminishes as the spacing decreases further. Consequently, an installation interval of approximately 50 m is recommended as the optimal configuration.

(4) The interconnection configuration of the internal grounding busbars significantly enhances safety by establishing a dense current dispersion network. Reducing the bonding interval from 200 m to 20 m resulted in a reduction of step voltage and touch voltage by 9.5% and 23.5%, respectively. To achieve a balance between cost-effectiveness and safety, it is recommended that the bonding interval for grounding busbars within the same compartment be set between 50 m and 80 m.

In summary, this study quantitatively analyzed the impact of multi-medium coupling on electrical characteristics, revealing the significant roles of the concrete shell shielding effect and layered soil. The findings indicate that vertical grounding electrodes exhibit a saturation trend in resistance reduction at approximately 50 m and identify the optimal efficacy range for grounding busbar bonding. Ultimately, this demonstrates that topology optimization based on saturation principles is significantly more effective in enhancing system safety than the indiscriminate increase of metal density.

ACKNOWLEDGEMENT

This work was supported in part by the National Engineering Research Center of UHV Technology and Novel Electrical Equipment Basis (No. NERCUHE-2024-KF-14).

REFERENCES

[1] Chen, Z. L., Z. F. Zhang, and H. F. Wang, "Current status and development trends of urban utility tunnel construction in China," *Tunnel Construction*, Vol. 45, No. 9, 1615–1626, 2025.

[2] Luo, B. C., "An investigation into the integrated construction of urban underground utility tunnels and roadways," *Civil Engineering*, Vol. 12, No. 2, 107–111, 2023.

[3] Zhao, X. Y., Y. G. Zhang, J. Z. Hong, *et al.*, "Analysis of 500 kV GIL tube grounding system," *Sichuan Electric Power Technology*, Vol. 43, No. 2, 59–62, 2020.

[4] Pires, C. L., S. I. Nabeta, and J. R. Cardoso, "ICCG method applied to solve DC traction load flow including earthing models," *IET Electric Power Applications*, Vol. 1, No. 2, 193–198, 2007.

[5] Charalambous, C. A., I. Cotton, and P. Aylott, "Modeling for preliminary stray current design assessments: The effect of crosstrack regeneration supply," *IEEE Transactions on Power Delivery*, Vol. 28, No. 3, 1899–1908, 2013.

[6] Charalambous, C. A. and P. Aylott, "Dynamic stray current evaluations on cut-and-cover sections of DC metro systems," *IEEE Transactions on Vehicular Technology*, Vol. 63, No. 8, 3530–3538, 2014.

[7] Bortels, L., A. Dorochenko, B. Van den Bossche, G. Weyns, and J. Deconinck, "Three-dimensional boundary element method and finite element method simulations applied to stray current interference problems. A unique coupling mechanism that takes the best of both methods," *Corrosion*, Vol. 63, No. 6, 561–576, 2007.

[8] Cerman, A., F. Janíček, and M. Kubala, "Resistive-type network model of stray current distribution in railway DC traction system," in *2015 16th International Scientific Conference on Electric Power Engineering (EPE)*, 364–368, Kouty nad Desnou, Czech Republic, 2015.

[9] Ibrahem, A., A. Elrayyah, Y. Sozer, and J. A. De Abreu-Garcia, "DC railway system emulator for stray current and touch voltage prediction," *IEEE Transactions on Industry Applications*, Vol. 53, No. 1, 439–446, 2017.

[10] Zaboli, A., B. Vahidi, S. Yousefi, and M. M. Hosseini-Biyouki, "Evaluation and control of stray current in DC-electrified railway systems," *IEEE Transactions on Vehicular Technology*, Vol. 66, No. 2, 974–980, 2017.

[11] Jabbehdari, S. and A. Mariscotti, "Distribution of stray current based on 3-dimensional earth model," in *2015 International Conference on Electrical Systems for Aircraft, Railway, Ship Propulsion and Road Vehicles (ESARS)*, 1–6, Aachen, Germany, Mar. 2015.

[12] Wang, Y. F., "Study on stray current interference range and monitoring method in metro depot," Ph.D. dissertation, China University of Mining and Technology, China, 2023.

[13] Yin, S., "Distribution of stray current in urban rail transit depot and the monitoring system design," *Urban Mass Transit*, Vol. 21, No. 7, 62–65, 2018.

[14] Song, D. Z., "Monitoring and control of stray current leakage in metro depot," *Urban Mass Transit*, Vol. 23, No. 7, 74–78, 2020.

[15] Zhu, F., J. Li, H. Zeng, and R. Qiu, "Influence of rail-to-ground resistance of urban transit systems on distribution characteristics of stray current," *High Voltage Engineering*, Vol. 44, No. 8, 2738–2745, 2018.

[16] Zhuang, H. X., F. Xu, W. X. Qian, *et al.*, "Concrete deterioration under coupling condition of stray current and salt-freezing," *Journal of the China Railway Society*, Vol. 44, No. 1, 143–152, 2022.

[17] Song, B., S. Wang, C. Xiang, X. Chen, and J. Tang, "Study on the influence of grounding resistance on cable fault overvoltage," *Energies*, Vol. 18, No. 10, 2601, 2025.

[18] Li, B., T. Gu, B. Li, and Y. Zhang, "Study on the gas-insulated line equivalent model and simplified model," *Energies*, Vol. 10, No. 7, 901, 2017.

[19] Tang, L., G. Liu, M. Wu, C. Zhao, X. Xu, and D. Huang, "Influence of GIL tube structure parameters on electrical characteristics of grounding system," *Power System Technology*, Vol. 43, No. 8, 3032–3038, 2019.

[20] Fan, R. Q., W. H. Zeng, B. Zou, *et al.*, "Study on grounding characteristics of transmission conduit corridors in challenging terrain," *Insulators and Surge Arresters*, 2024 (in Chinese).

[21] Pan, W. X., T. C. Liu, B. Wang, and D. Min, "Grounding computation method for layered-soil with arbitrary massive texture foundation," *Transactions of China Electrotechnical Society*, Vol. 31, No. 7, 145–151, 2016.

[22] Li, C., X. Chen, C. He, H. Li, and X. Pan, "Alternating current induced corrosion of buried metal pipeline: A review," *Journal of Chinese Society For Corrosion and Protection*, Vol. 41, No. 2, 139–150, 2021.

[23] Yang, Y. T., "Research on concrete resistivity and reinforcing concrete steel corrosion rate," Ph.D. dissertation, Dalian University of Technology, Dalian, China, 2009.